ACS APPLIED MATERIALS & INTERFACES

RESEARCH ARTICLE

www.acsami.org

# Ultrafast Coloring-Bleaching Performance of Nanoporous $WO_3-SiO_2$ Gasochromic Films Doped with Pd Catalyst

Dezeng Li,[†] Guangming Wu,[*,‡] Guohua Gao,[‡] Jun Shen,[‡] and Fuqiang Huang[*,†]

[†]CAS Key Laboratory of Materials for Energy Conversion and State Key Laboratory of High Performance Ceramics and Superfine Microstructure, Shanghai Institute of Ceramics, Chinese Academy of Sciences, Shanghai 200050, P. R. China

[‡]Department of Physics, Tongji University, Shanghai 200090, P. R. China

Supporting Information

**ABSTRACT:**

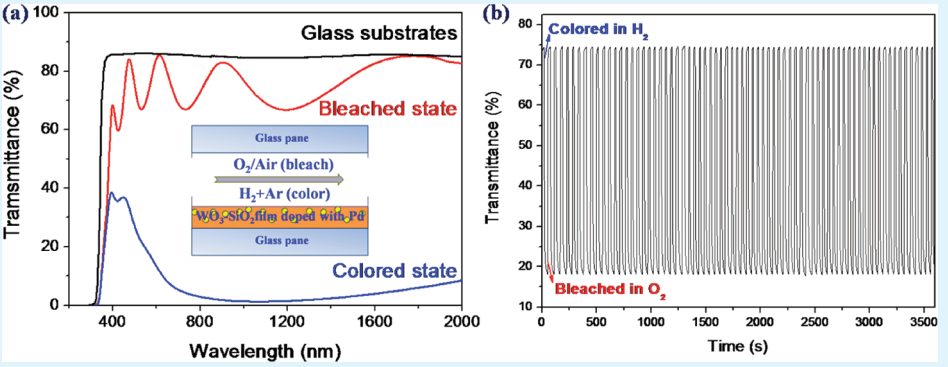


The gasochromic performance and durability of $WO_3$-based films can be improved by doping $SiO_2$ particles within $WO_3$ matrix forming nanoporous supporting network and dispersing Pd catalyst inside films with enhanced catalytic activity. Nanoporous $WO_3-SiO_2$ composite films loaded with Pd catalyst were prepared by sol−gel dip-coating process and served as an active chromogenic layer to fabricate a double-glazed gasochromic device. The structure, morphology, optical properties and gasochromic performance of $WO_3-SiO_2$ films were fully investigated. The $WO_3-SiO_2$ films exhibit excellent gasochromic performance with ultrafast coloring rate of 14.8% per second (%/s) ($WO_3$: 2.84%/s) and bleaching rate of 44.1%/s ($WO_3$: 7.18%/s). The transmittance changed between 17.8 and 74.6% during coloring-bleaching cycles, and totally reversibility and stability were achieved.

**KEYWORDS:** gasochromic, coloring-bleaching, $WO_3-SiO_2$ films, sol−gel process, nanoporous structure

## 1. INTRODUCTION

Gasochromic switchable films based on tungsten trioxide ($WO_3$) offer a wide variety of promising applications in smart windows,[1−4] antidazzling mirrors,[5] displays,[6,7] and hydrogen sensors[8,9] because of their simpler structure, lower costs, and excellent optical switching response. $WO_3$-based films with thin layer of catalyst (Pt, Pd) can be prepared by sputtering,[10−13] electrodeposition,[14,15] pulsed laser deposition,[16,17] and sol−gel method with high process speed, low cost, and continuous production.[4,18−21]

The coloring-bleaching performance and durability of gasochromic $WO_3$ films play a vital role in practical applications, which are related to the microstructure of films and the activity of catalyst.[8,22] Repeated coloring-bleaching process and long-term storing usually lead to structural collapse and densification and catalyst poisoning, which increases switchable time and results in partial gasochromic irreversibility.[23] Composite films with nanoporous structure and enhanced mechanical and thermal stability are a promising way to improve the gasochromic performance. Doping catalyst nanoparticles by adding adjustable metal salt into sol matrix via sol−gel process is an alternative approach to ensure catalytic activity. Moreover, the gasochromic films are unsuccessfully applied for the insufficient response of switchable time on the order of minutes.[24] The improvement of gasochromism of $WO_3$-based films remains a great challenge.

In this paper, nanoporous $WO_3-SiO_2$ composite films were prepared on the surface of glass substrates by sol−gel dip-coating process. The Pd catalyst was introduced by adding $PdCl_2$ into precursor sol matrix. Structure, morphology, optical properties and gasochromic performance of composite films were fully investigated. The $WO_3-SiO_2$ films exhibited high gasochromic performance with ultrafast coloring-bleaching rates and excellent reversibility and stability. The underlying reasons of the improvement of gasochromic performance were also discussed.

**Received:** June 17, 2011
**Accepted:** July 25, 2011
**Published:** July 25, 2011

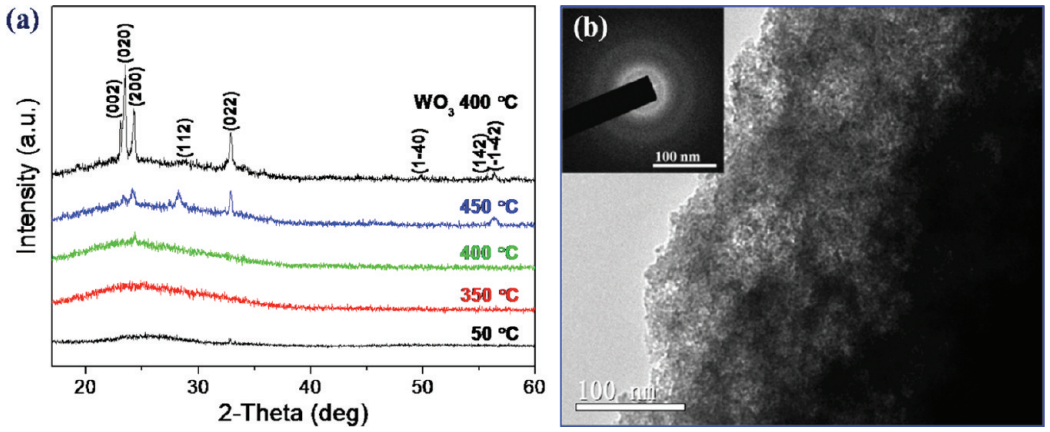


**Figure 1.** (a) XRD patterns of $WO_3-SiO_2$ films annealed at 50, 350, 400, and 450 °C, and $WO_3$ films annealed at 400 °C; (b) TEM image of as-prepared $WO_3-SiO_2$ films (inset: selected-area electron diffraction pattern).

## 2. EXPERIMENTAL SECTION

All chemical reagents in the experiment were purchased from Sinopharm Chemical Reagent Co. Ltd. and used without further purification. W powder (99.9%) and $H_2O_2$ (30%) with a molar ratio of 1:3 were added into ethanol solution under ice bath conditions, followed by stirring for 1 h and centrifugation. A transparent precursor sol of 0.3 mol $L^{-1}$ W was obtained after a certain amount of ethanol was added to adjust the concentrations of W. $PdCl_2$ was added into $WO_3$ precursor sol with an optimized molar ratio of Pd:W = 1:50. The silica sol with a concentration of 0.4 mol $L^{-1}$ was synthesized using tetraethyl orthosilicate (TEOS, 208.33, AR) as precursor, ammonia as catalyst and ethanol as solvent with a molar ratio of 1:2:40.[25] The $WO_3-SiO_2$ precursor sols were prepared by adding silica sols into $WO_3$ precursor sols under stirring condition with optimized concentration of 30 v/v%, which is stable over 6 months in refrigerator. The uniform $WO_3-SiO_2$ films were obtained by dip-coating the precursor sols on glass slide substrates (typically 75 by 25 mm and 1 mm thick) at a controlled speed range of 3−200 mm/min (Dip Coater, MTI Co., China), followed by drying at 50 °C for 60 min. The $WO_3$ films were also prepared on glass substrates for comparison according to the same route.

The crystalline structure was characterized by X-ray diffraction (XRD, Bruker D8). Refractive index and thickness of films were measured by ellipsometer (SC620UVN). Structure of sols and films was examined by transmission electron microscopy (TEM, JEM2100F). Surface morphology of films was investigated by field emission scanning electron microscopy (FE-SEM, Hitachi S-4800) and atomic force microscopy (AFM, XE100). A spectrophotometer (Hitachi U4100) was used to record transmittance spectra of films and optical transmittance response as a function of time at 700 nm.

## 3. RESULTS AND DISCUSSION

The crystalline structure of $WO_3-SiO_2$ films annealed at different temperatures was characterized. According to the XRD patterns shown in Figure 1a, the triclinic phase of $WO_3$ (JCPDS 20−1323) can be indexed. Only several weak diffraction peaks were observed when the $WO_3-SiO_2$ films were annealed at 450 °C, where the crystallization of $WO_3$ films occurred at 400 °C. The crystal sizes of $WO_3-SiO_2$ and $WO_3$ films were calculated by Scherrer equation to be ∼29 and ∼47 nm, respectively. The existence of $SiO_2$ particles in $WO_3$ matrix leads to the formation of smaller crystal size and the improvement of crystal temperature. The TEM image and selected-area electron diffraction pattern of as-prepared $WO_3-SiO_2$ films in Figure 1b show the nanoporous and amorphous structure, which matches the results of XRD.

Because of the excellent mechanical and thermal stability of $SiO_2$, the durability of gasochromic films could be improved by doping $SiO_2$. Figure 2 shows the SEM images of $WO_3-SiO_2$ and $WO_3$ films annealed at 50 and 450 °C, respectively. It is observed that the $WO_3-SiO_2$ film consists of agglomerated nanoparticles and pores (Figure 2a), and the $WO_3$ film has granular nanoporous microstructure and flat texture (Figure 2c). After annealing treatment at 450 °C, no clear collapse and densification was observed in $WO_3-SiO_2$ film (Figure 2b), however, the $WO_3$ film became dense and more flat (Figure 2d), which means the nanoporous structure of $WO_3-SiO_2$ film was maintained during annealing process due to existence of $SiO_2$ particles.

The microstructure of gasochromic films is easily influenced by the gasochromic reaction and the long-term storing environment. The water from coloring-bleaching reaction and ambient partially achieved the surface of films and combined with $WO_3$ particles during aging process. When the water was desorbed from the surface of films, the superficial nanostructure was destroyed and bigger agglomerates of particles were formed due to great surface tension of water. The AFM images in Figure 3 exhibit the morphology of $WO_3-SiO_2$ and $WO_3$ films as prepared and colored for 30 times. From images a and b in Figure 3, it seems that the microstructure of $WO_3-SiO_2$ composite film was not obviously affected during the gasochromic process, where the roughness (rms) was 0.71 and 0.82 nm before and after gasochromic process, respectively. However, the $WO_3$ films appear flat patterns on the surface and structural collapse and densification, where the rms changed from 0.74 to 0.27 nm (Figure 3c,d). Therefore, the durability of composite films was demonstrates by introducing $SiO_2$.

The coloration of gasochromic devices takes place under $H_2$/Ar exposure ($H_2$: 4%) from a transparent state to a colored state (usually blue) resulting in decreased transmittance and the bleaching happens by exposure of devices to $O_2$ or air during a reversible process. The gasochromic performance of $WO_3-SiO_2$ films is dependent on the content of dopants and the thickness of films, which was optimized with a result of 30% $SiO_2$ content and about 415.5 nm thickness. Figure 4a shows the typical transmittance spectra of $WO_3-SiO_2$ films at both colored and bleached states and the inset gives the schematic diagram of a gasochromic

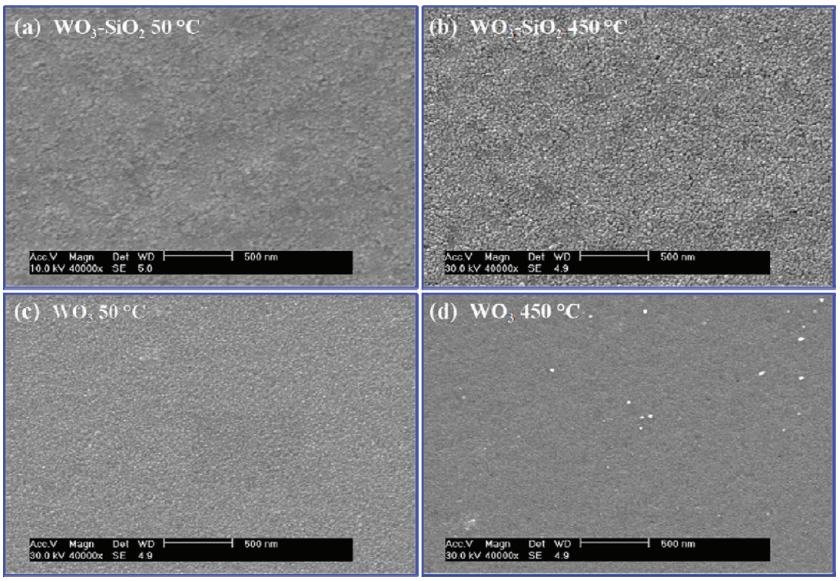


**Figure 2.** SEM images of (a, b) $WO_3-SiO_2$ and (c, d) $WO_3$ films annealed at (a, c) 50 and (b, d) 450 °C.

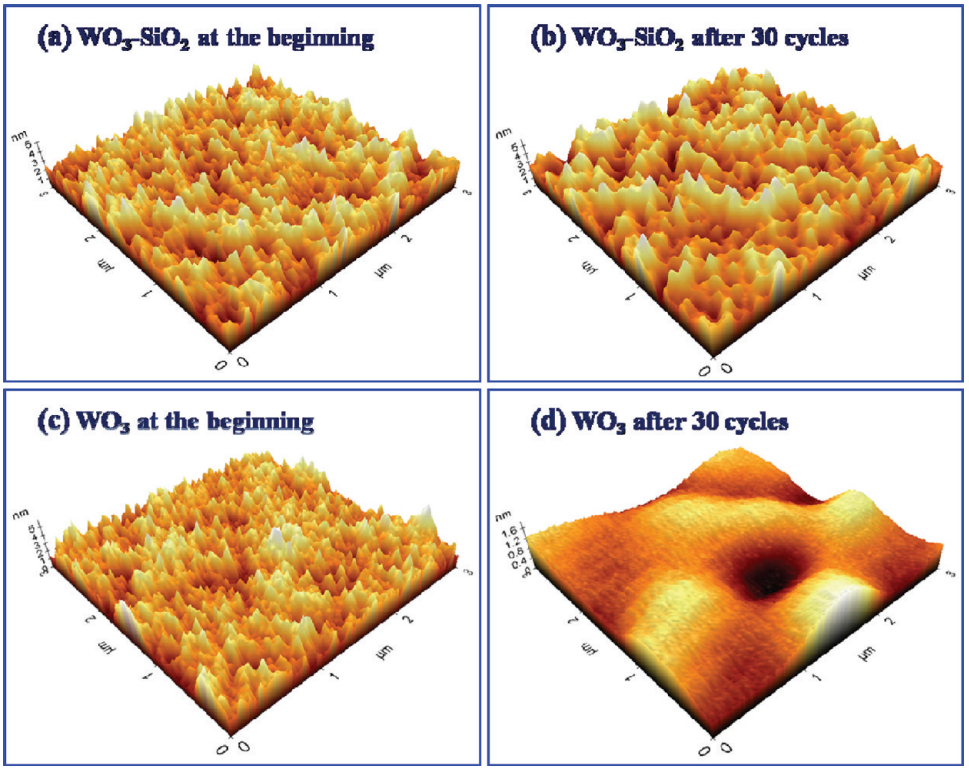


**Figure 3.** AFM images of (a, b) $WO_3-SiO_2$ and (c, d) $WO_3$ films: (a, c) as-prepared and after (b, d) 30 coloring-bleaching cycles.

device with double-glazed middle-empty structure, consisting of a Pd catalyst doped $WO_3-SiO_2$ film.

The optical constants, such as refractive index ($n$), play an important role in design and research of gasochromic films, and also can provide the information of structure of films. The dependence of $n$ of $WO_3$-based films on contents of $SiO_2$ were investigated, as shown in Figure 4b. $n$ of $WO_3$ film is 1.91 and as the content of $SiO_2$ increased, $n$ decreased to 1.79 for the $WO_3$ film with 30% $SiO_2$. The decrease of $n$ of composite films arises from the introducing of amorphous $SiO_2$ dopants with low $n$ (~1.45) and the formation of nanoporous structure.

The gasochromic performance of $WO_3-SiO_2$ and $WO_3$ films was investigated to certify the influence of $SiO_2$ dopants on coloring-bleaching process of films. Figure 5 exhibits the normalized transmittance of the films as a function of reaction time, where the ordinate was defined as the transmittance logarithm of films. The coloring ($R_c$) and bleaching ($R_b$) rates were calculated as the linear slope of transmittance ratio vs reaction time curve by

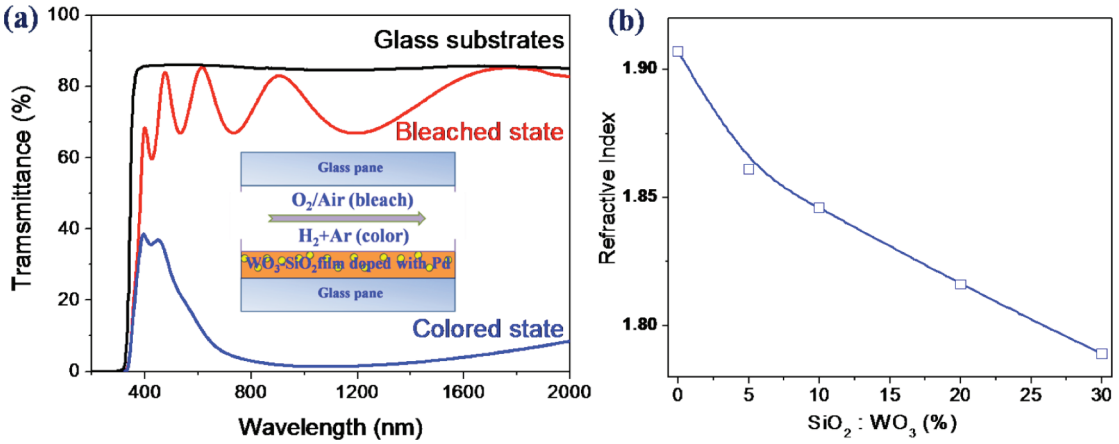


**Figure 4.** (a) Typical transmittance spectra of $WO_3-SiO_2$ films with thickness of about 415.5 nm at bleached and colored states (inset: schematic diagram of gasochromic device consisting of Pd doped $WO_3-SiO_2$ film). (b) Refractive index of composite films with various amounts of $SiO_2$.

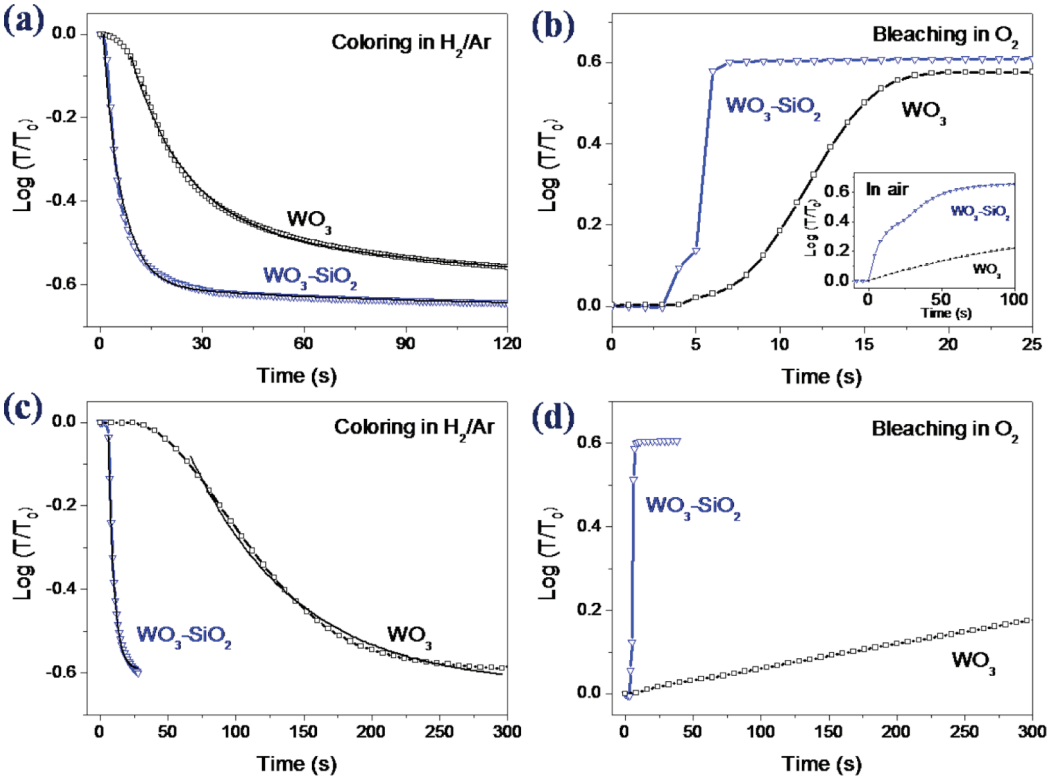


**Figure 5.** Coloring and bleaching kinetics of $WO_3-SiO_2$ and $WO_3$ films (a, b) as-prepared and (c, d) after 30 coloring-bleaching cycles. The films (a, c) colored in $H_2$/Ar mixture (the black solid lines as exponentially fitting curves) and (b, d) bleached in $O_2$ (inset in b: the films bleached in air).

following formula:[24,26]

$$R_c = \frac{(T_c - T_{c0})}{t_c - t_{c0}} \quad (1)$$

$$R_b = \frac{(T_b - T_{b0})}{t_b - t_{b0}} \quad (2)$$

where $T_{c0}$ and $T_{b0}$ are the initial transmittance ratios of colored and bleached states, respectively, and $T_c$ and $T_b$ are the final transmittance ratios, and $t_{c0}$, $t_{b0}$, $t_c$, and $t_b$ are the reaction time associated with those ratios. The coloring and bleaching rates are expressed as a percentage of transmittance per second (%/s). The as-prepared $WO_3-SiO_2$ and $WO_3$ films exhibit fast coloring and bleaching kinetics, as shown in Figure 5a,b. The coloring rate of $WO_3-SiO_2$ films is about 14.8%/s and fully coloration was obtained in 15 s. It is foreseeable the time to reach a full coloration can diminish to be less than 15 s when pure $H_2$ replaces $H_2$/Ar mixture. The coloring rate of $WO_3$ films is about 2.84%/s and saturation was achieved in 60 s. The bleaching rates of $WO_3-SiO_2$ and $WO_3$ films are 44.1%/s and 7.18%/s, respectively, where ultrafast reaction kinetics was demonstrated in $WO_3-SiO_2$ films. These films were exposed to air to compare the influence of $O_2$ concentrations on the bleaching process.

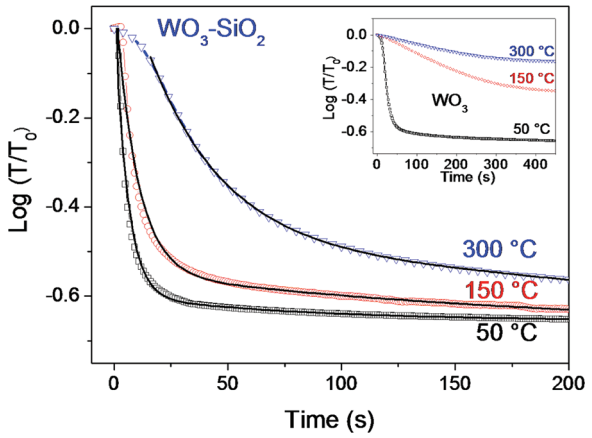


**Figure 6.** Coloring kinetics of $WO_3-SiO_2$ annealed at 50, 150, and 300 °C, and the black solid lines as exponentially fitting curves. (Inset: $WO_3$ films annealed at 50, 150, and 300 °C).

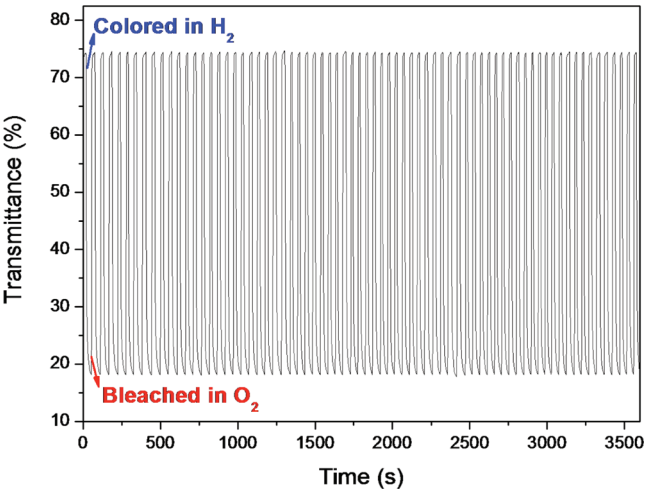


**Figure 7.** Coloring−bleaching cycles of $WO_3-SiO_2$ films colored in $H_2$/Ar and bleached in $O_2$.

It is found that the bleaching rate of $WO_3$ films changed into slower and was only 0.19%/s, and that of $WO_3-SiO_2$ films was 1.95%/s, which was comparable with the values of $WO_3$ films in pure $O_2$. After 30 coloring-bleaching cycles (Figure 5c,d), the gasochromic kinetics of $WO_3$ turned to be very slow, and the coloring and bleaching rates were calculated to be 0.55%/s and 0.066%/s, respectively. The $WO_3-SiO_2$ films retained ultrafast coloring-bleaching kinetics during gasochromic process (coloring rate: 14.2%/s, bleaching rate: 41.6%/s). The fitting coloration curves of $WO_3-SiO_2$ and $WO_3$ films at the beginning and after 30 cycles were given in Figure 5(a,c) as the black solid lines. The fitting function used is as follows: $y = A\exp(-x/\tau) + B$, where $A$ and $B$ are constants, and $\tau$ is the exponentially decaying time constant. The $\tau$ of $WO_3-SiO_2$ film at the beginning and after 30 cycles is 4.2 and 5.5 s, and that of $WO_3$ film are 15.2s and 79.1s, respectively. The microstructure of $WO_3$ films became collapsed and the pores in $WO_3$ films were partially blocked, determined in AFM results, which was against the further absorption of gas along with the reactive process and thus lead to the gradually slower coloring rate. The reaction rates of gasochromic process were greatly improved and the gasochromic stability was maintained by $SiO_2$ doping.

The gasochromic performance of $WO_3-SiO_2$ and $WO_3$ films annealed at 150 and 300 °C for 60 min was determined and the logarithm curves of transmittance as a function of reaction time are shown in Figure 6. After annealing treatment, the coloration of $WO_3-SiO_2$ films slowed; however, fast coloring rates of 11.2%/s (150 °C) and 1.36%/s (300 °C) were achieved. The $\tau$ is 4.2 s (50 °C), 9.4 s (150 °C), and 32.6 s (300 °C) from the fitting curves. The $WO_3$ films are easily affected by annealing treatment, as shown in the inset in Figure 6. The $WO_3$ films colored very slowly after annealing at 150 °C with a rate of 0.058%/s, more than 480 s required achieving the full coloration, and the coloring rate of films annealed at 300 °C slowed down to 0.029%/s, revealing the obvious change of the microstructure of films. During annealing process, the $WO_3$ films become denser, which leads to smaller pore volumes and decreased inner surface area, demonstrated in SEM results, and the enhanced crystallization of $WO_3$ films weakens the diffusion of gas atoms. The amorphous structure is advantageous for gas diffusion and gasochromic reaction because of the existing inner pores and the large surface area of films. The microstructure of $WO_3-SiO_2$ films was not obviously influenced by annealing treatment and thus fast gasochromic performance was maintained, which is attributed to the doped $SiO_2$ serving as supporting framework.

To show the reversibility and stability of gasochromic process, we plotted the transmittance spectra of $WO_3-SiO_2$ films colored in $H_2$/Ar and bleached in pure $O_2$ as a function of reaction time in Figure 7. The composite films show excellent and stable gasochromic performance: a) gasochromic rates, 72 coloring-bleaching cycles in 3600 s; b) the transmittance changed between 17.8 and 74.6%, responding to coloring-bleaching cycles with a contrast of 56.8%; c) the transmittance of colored and bleached states almost reached the same values as their previous ones, which demonstrates the totally reversibility and stability of gasochromic process. The transmittance of gasochromic cycles of $WO_3-SiO_2$ films and $WO_3$ films (about 402.6 nm) was plotted against time in supporting materials. For $WO_3-SiO_2$ films, more than 120 cycles appeared in 7200 s. However, only 18 cycles appear in 10 000 s for $WO_3$ films and both colored and bleached rates became slower, i.e., 280 s for the first cycle and 1000 s for the last cycle.

There are two widely accepted models: double injection model,[10,27,28] and oxygen vacancies-color center model.[3,12,19] In the former model, cations ($H^+$, $Li^+$, $Na^+$) and electrons are simultaneously injected into a $WO_3$ film and reduce $W^{6+}$ to $W^{5+}$, forming tungsten bronze ($H_xWO_3$). In the latter model, dissociated hydrogen by catalyst is transferred into a pore or grain boundary of $WO_3$ and subsequently creates water and an oxygen vacancy. In these two models, the gasochromic performance affected by ion injection or atom diffusion is related to the microstructure of $WO_3$ based films and distribution of catalyst in films. The improvement of gasochromic performance can be discussed concerning the influence of $SiO_2$ dopants on the microstructure of films and the effect of doped Pd particles on the reaction process.

The doping of $SiO_2$ within $WO_3$ matrix forming nanoporous supporting network with high specific surface area increases interface, and accelerates the diffusion of atoms, and maintains the stability of microstructure of films. It is facile to form network of nanoparticles in silica sols in basic condition where the condensation of particles is faster than TEOS hydrolysis.[29] When $WO_3$ precursor sols and silica sols were homogeneously mixed, the porous cluster microstructure of $WO_3-SiO_2$ composite sols

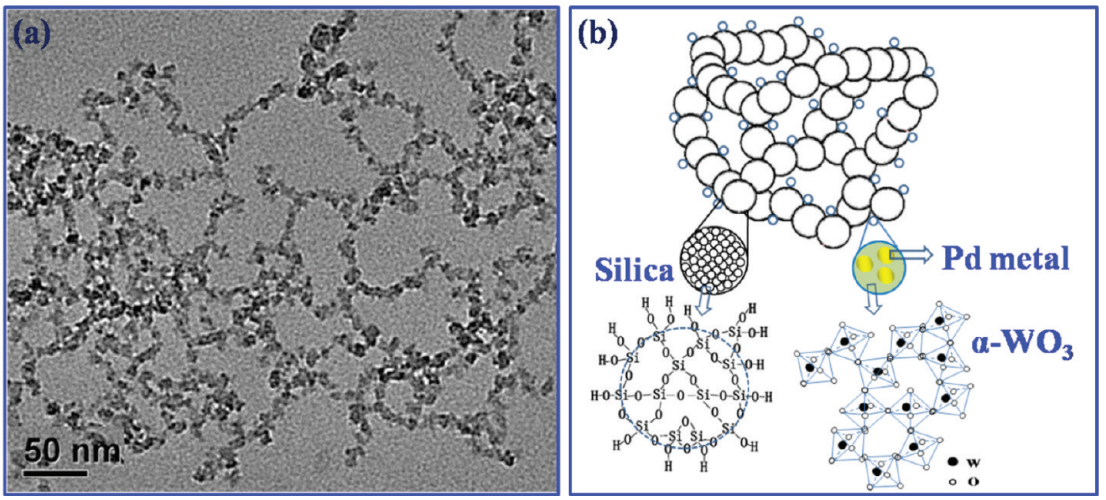


**Figure 8.** (a) TEM micrographs of $WO_3-SiO_2$ sols loaded with Pd catalyst. (b) The schematic diagram of $WO_3-SiO_2$ composite structure.

was obtained and shown in Figure 8a. An obvious particulate network was formed in the sols, and the cross-link microstructure was stable during several months. The approximate average particle diameter of the sol is 10 nm and the interspaces responding to the pore of films have an average size about 50 nm. Based on the results of microstructure of composite sols and films, the schematic diagram of $WO_3-SiO_2$ structure is present in Figure 8b. The $WO_3$ grains with amorphous structure loaded with Pd catalyst are around the $SiO_2$ network as a supporting framework to form nanoporous and stable composite structure.

The distribution of doped catalyst inside films may take advantageous over the thin catalyst layer deposited only on the surface of films to improve the catalytic activity and to avoid the poisoning of catalyst during aging process. The poisoning of catalyst increases the time of adsorption, dissociation and coloring-bleaching reaction, and leads to partially irreversibility. The existence of doped Pd catalyst with nanosize dimension inner films via sol−gel process increases the effective reaction surface and can enhance the reversibility by reacting with residual $H_2$ or $O_2$ not all dissociated on the surface. The protection of doped catalyst can be improved by films when exposed to environment for a long time. Furthermore, the Pd nanoparticles loaded in films may possess surface plasma resonance effect to ensure the ultrafast coloring-bleaching performance.

## 4. CONCLUSIONS

The gasochromic devices consisting of a nanoporous $WO_3-SiO_2$ film doped with Pd catalyst were fabricated via sol−gel dip-coating process. The structure, morphology, optical properties and gasochromic performance of $WO_3-SiO_2$ films were fully investigated. The influence of $SiO_2$ doping on microstructure, gasochromic performance and durability of $WO_3$ based films was determined.

The $WO_3-SiO_2$ films show excellent gasochromic performance with ultrafast coloring-bleaching rates and totally reversibility and stability. The coloring rate of $WO_3-SiO_2$ films is 14.8%/s and bleaching rate is 44.1%/s in pure $O_2$ (1.95%/s in air), where the coloring rate of $WO_3$ films is 2.84%/s and bleaching rate is 7.18%/s in pure $O_2$ (0.19%/s in air). After tens of coloring-bleaching cycles, the performance of $WO_3$ turned to be very slow and the $WO_3-SiO_2$ films retained ultrafast gasochromic kinetics.

The underlying reasons of the improvement of gasochromic performance are discussed and are attributed to three facets: a) the amorphous structure with large specific surface area and plentiful diffusion channels; b) the existence of $SiO_2$ particles within $WO_3$ matrix forming nanoporous supporting network; c) the distribution of Pd catalyst doped inner films with improved catalytic activity.

## ■ ASSOCIATED CONTENT

**Supporting Information.** Additional information, figures, and tables (PDF). This material is available free of charge via the Internet at http://pubs.acs.org.

## ■ AUTHOR INFORMATION

**Corresponding Author**

*Tel.: +86-21-5241-1620. Fax: +86-21-5241-6360. E-mail: huangfq@mail.sic.ac.cn (F.H.); wugm@tongji.edu.cn (G.W.).

## ■ ACKNOWLEDGMENT

Financial support from National 973 Program of China Grants (2009CB939903 and 2007CB936704), National scientific and technological support project (2009BAC62B02), National Science Foundation of China Grants (50772123, 20901083 and 50902143) and Science and Technology Commission of Shanghai Grants (08JC1420200 and 0952 nm06500) are gratefully acknowledged. The authors thank Prof. Bin Zhou and Dr. Zhihua Zhang of Tongji University for helpful discussions and Dr. Jichao Shi and M.S. Shiwen Chen of Tongji University for AFM and partial optical measurements.

## ■ REFERENCES

(1) Granqvist, C. G. *Adv. Mater.* **2003**, *15*, 1789–1803.
(2) Feng, M.; Pan, A. L.; Zhang, H. R.; Li, Z. A.; Liu, F.; Liu, H. W.; Shi, D. X.; Zou, B. S.; Gao, H. *Appl. Phys. Lett.* **2005**, *86*, 141901.
(3) Wittwer, V.; Datz, M.; Ell, J.; Georg, A.; Graf, W.; Walze, G. *Sol. Energy Mater. Sol. Cells* **2004**, *84*, 305–314.
(4) Krašovec, U. O.; Topic, M.; Georg, A.; Draciz, G. *J. Sol−Gel Sci. Technol.* **2005**, *36*, 45–52.
(5) Naseri, N.; Azimirad, R.; Akhavan, O.; Moshfegh, A. Z. *J. Phys. D: Appl. Phys.* **2007**, *40*, 2089–2095.

(6) Cui, X.; Zhang, H.; Dong, X.; Chen, H.; Zhang, L.; Guo, L.; Shi, J. *J. Mater. Chem.* **2008**, *18*, 3575–3580.
(7) Deepa, M.; Saxena, T. K.; Singh, D. P.; Sood, K. N.; Agnihotry, S. A. *Electrochim. Acta* **2006**, *51*, 1974–1989.
(8) Chan, C. C.; Hsu, W. C.; Chang, C. C.; Hsu, C. S. *Sens. Actuators, B* **2010**, *145*, 691–697.
(9) Cao, B.; Chen, J.; Tang, X.; Zhou, W. *J. Mater. Chem.* **2009**, *19*, 2323–2327.
(10) Shanak, H.; Schmitt, H.; Nowoczin, J.; Ziebert, C. *Solid State Ionics* **2004**, *171*, 99–106.
(11) Stolze, M.; Gogova, D.; Thomas, L. K. *Thin Solid Films* **2005**, *476*, 185–189.
(12) Georg, A.; Graf, W.; Neumann, R.; Wittwer, V. *Sol. Energy Mater. Sol. Cells* **2000**, *63*, 165–176.
(13) Shim, J. Y.; Lee, J. D.; Jin, J. M. *Sol. Energy Mater. Sol. Cells* **2009**, *93*, 2133–2137.
(14) Krasnov, Y. S.; Kolbasov, G. Y. *Electrochim. Acta* **2004**, *49*, 2425–2433.
(15) Feng, J. J.; Xu, J. J.; Chen, H. Y. *Electrochem. Commun.* **2006**, *8*, 77–82.
(16) Soto, G.; Cruz, W. D. L.; Diaz, J. A.; Machorro, R.; Castillo, F. F.; Farias, M. H. *Appl. Surf. Sci.* **2003**, *218*, 282–290.
(17) Ranjbar, M.; Garavand, N. T.; Mahdavi, S. M. *Sol. Energy Mater. Sol. Cells* **2010**, *94*, 201–206.
(18) Xu, X. Q.; Shen, H.; Xiong, X. Y. *Thin Solid Films* **2002**, *415*, 290–295.
(19) Orel, B.; Krašovec, U. O.; Grošelj, N.; Kosec, M.; Drazic, G.; Reisfeld, R. *J. Sol-Gel Sci. Technol.* **1999**, *14*, 291–308.
(20) Sekimoto, S.; Nakagawa, H.; Okazaki, S.; Fukuda, K.; Asakura, S.; Shigemori, T.; Takahashi, S. *Sens. Actuators, B* **2000**, *66*, 142–145.
(21) Li, J.; Zhao, Q.; Zhang, G. *Solid State Sci.* **2010**, *12*, 1393–1398.
(22) Ghosh, R.; Baker, M. B.; Lopez, R. *Thin Solid Films* **2010**, *518*, 2247–2249.
(23) Baetens, R; Jelle, B. P.; Gustavsen, A. *Sol. Energy Mater. Sol. Cells* **2010**, *94*, 87–105.
(24) Vitry, V.; Renaux, F.; Gouttebaron, R.; Dauchot, J. P.; Hecq, M. *Thin Solid Films* **2006**, *502*, 265–269.
(25) Li, D. Z.; Huang, F. Q.; Ding, S. J. *Appl. Surf. Sci.* (DOI: 10.1016/j.apsusc.2011.05.126).
(26) Shanak, H.; Schmitt, H. *Phys. Status Solidi A* **2006**, *203*, 3748–3753.
(27) Lee, S. H.; Cheong, H. M.; Liu, P.; Smith, D.; Tracy, C. E.; Masarenhas, A.; Pitts, J. R.; Deb, S. K. *Electrochim. Acta* **2001**, *46*, 1995–1999.
(28) Subrahmanyam, A.; Karuppasamy, A. *Sol. Energy Mater. Sol. Cells* **2007**, *91*, 266–274.
(29) Wu, G.; Wang, J.; Shen, J. *Mater. Res. Bull.* **2001**, *36*, 2127–2139.